

## SOME NEW DIRECTIONS IN IMPEDANCE SPECTROSCOPY DATA ANALYSIS

JAMES ROSS MACDONALD

Department of Physics and Astronomy, University of North Carolina, Chapel Hill, NC 27599-3255, U.S.A.

(Received 10 March 1993)

**Abstract**—New developments in two main data analysis areas are discussed: (a) complex nonlinear least squares (CNLS) fitting of data and (b) data-transforming and optimizing integral transforms. In the first category, a Monte Carlo study is used to answer the question of which of several different parameterizations of an ambiguous equivalent circuit model lead to minimum correlation between fitting parameters, a desirable condition. In addition, results are briefly discussed which address the questions of (1) what should be minimized in CNLS fitting? (2) how well can one discriminate between exact small-signal binary electrolyte response and conventional finite-length diffusion response? and (3) what is the ultimate precision of parameter estimates obtained in a CNLS fit? In the second area, new forms of the Kronig-Kramers relations (KKR) are discussed; the accuracy of several different ways of carrying out the numerical quadratures needed in such transforms is compared; and it is shown how random errors present in complex data are transformed by the KKR. Then, new transforms are described and illustrated that can replace exponential Fourier and KK transforms and, at the same time, can greatly reduce random error and some kinds of systematic errors in real, imaginary, or complex frequency response data or transient response data without the need for smoothing or filtering parameter choices.

**Key words:** impedance spectroscopy, data analysis, integral transforms.

### INTRODUCTION

I summarize three recent developments and describe new results of interest to impedance spectroscopy (IS). The first four topics concern improvements in complex nonlinear least squares (CNLS) fitting, and they employ the updated LEVM CNLS fitting program, version 5.0[1-3]. The remaining topics deal with noise transformation in Kronig-Kramers (KK) transforms and with new ways to perform optimizing integral transforms which are functionally equivalent to ordinary KK and Fourier transforms but, unlike these transforms, greatly reduce noise and other errors in the data.

### TOPICS IN COMPLEX NONLINEAR LEAST SQUARES FITTING

#### *Minimum correlation in ambiguous situations: Alternate parameterizations*

In addition to the ambiguity associated with alternate but electrically equivalent ways of connecting a set of ideal  $R$ ,  $L$  and  $C$  circuit elements in various configurations[1], ambiguity arises from the various possible ways of parameterizing a composite circuit element such as the  $ZC$  (Cole-Cole response at the  $Z$  level[1, 4]). Is one such parameterization to be preferred to another in CNLS fitting of IS data? Here, I examine this question for a common situation by means of Monte Carlo (MC) data fitting. The smaller the correlations between free parameters in a CNLS fit, the better these parameters can be esti-

ated. Thus, usually that specific parameterization which leads to the lowest correlations should be preferred to others.

But a difficulty arises. When one carries out such a fit on data containing measurement errors, one obtains only a single estimate of the parameter correlation matrix. No estimate is then available of the uncertainty of the correlations and of whether the particular set of values found is representative of the actual situation or is perhaps quite unrepresentative. Furthermore, the correlation values found from a CNLS fit with a computer program like LEVM are based on a final linearization of the problem around the converged values of the parameters. Such linearization can often lead to appreciable errors for a fitting model nonlinear in some free parameters, the usual case in the IS area. To resolve this problem, Monte Carlo simulation is suitable. By generating a large number,  $K$ , of fits of a given circuit (usually  $K > 100,000$ ), each with a different set of random errors, one can obtain for comparison well-determined estimates of both linearized correlations and those calculated directly from the MC results.

In order to illustrate the problem and to shed some light on its solution, I investigated the MC response of the  $ZC$  frequency response function, written in the general form

$$Z(\omega) = Z'(\omega) + iZ''(\omega) = A/[1 + (i\omega B)^n]. \quad (1)$$

When  $-Z''(\omega)$  is plotted in the complex plane vs.  $Z'(\omega)$  for a sufficiently large range of  $\omega$  values, the result is a semicircle with its center depressed below

the  $Z'$  real axis if  $\psi < 1$ . To begin with, the quantities  $A \equiv R$ , a resistance, and  $B \equiv \tau$ , a relaxation time, were set to unity;  $\psi$  was fixed at 0.5; and  $N = 49$  exact data points were calculated for the range  $0.001 \leq \omega \leq 1000$ , with eight points per decade distributed uniformly in  $\log(\omega)$ . These exact values were then used in the MC generation of data with proportional errors[2].

In all the MC simulations reported here, Gaussian errors with zero mean and the same standard deviation were used in generating data with either additive or proportional random errors. Let  $N(0, \sigma, I_j) = \sigma N(0, I_j)$  represent an independent random sample drawn from a normal distribution with zero mean and a homoscedastic standard deviation (SD) of  $\sigma_r$ . Here  $I_j$ , an element of the unit vector, is unity for all  $1, 2 \dots, N$  values of  $j$ . It will be convenient in some of the following discussion to replace  $Z(\omega)$  by  $F(\omega) = F'(\omega) + iF''(\omega)$  in order to indicate that the methods apply not just to impedances and admittances, but to any real and imaginary functions of frequency. Now we can construct "experimental" MC  $F'$  data with errors by means of the relation

$$F'_m(\omega_j) = F'_{ex}(\omega_j)[1 + \beta\sigma_r N(0, I_j)] + (1 - \beta)\sigma_r N(0, I_j), \quad (2)$$

where  $F'_{ex}$  is the error-free part of  $F'_m$ , and  $\beta = 1$  for proportional random errors and  $\beta = 0$  for additive ones. A similar expression with different or the same  $N(0, I_j)$  values may be written for  $F''_m(\omega_j)$ . It follows that if the asymptotic SD of  $F'_m$  is defined as  $S$ , the corresponding relative standard deviation (RSD), sometimes called the coefficient of variation,  $S/\langle F'_m \rangle$ , which is equal to  $S/F'_{ex}$  if bias is absent, is just  $\sigma_r$  for  $\beta = 1$ . The choice of  $\sigma_r = 0.02$ , for example, leads to random proportional errors with a SD of 0.02, which is not the same as a fixed 2% error for all values of  $F'_m$ . In these MC calculations, not only are random errors different for each of the  $N$  values of  $j$ , but they are also different for each of the  $K$  replications.

Table 1 defines the seven different parameterizations of  $A$  and  $B$  which were investigated. Here, the choices made for  $A$  and  $B$  are shown; the corresponding choices are given for the free parameters  $\theta_1$  and  $\theta_2$ ; and the no-error values of these parameters for the data used are listed in the last two columns. The conventional angle  $\chi$  is given by  $(\pi/2)\psi$ , and the parameter  $\psi$  was taken either free to vary during the CNLS fitting or was fixed at 0.5. Note that  $\tau/C$  has the dimensions of a resistance,

and (since  $R$  is here the DC value of  $Z'$ )  $R_0$  is the diameter of the corresponding  $\psi = 1$  semicircle, appropriate for an undistributed situation. When  $\psi < 1$  and thus  $R \equiv R_0 \sin(\chi) < R_0$ , one is concerned with a distribution of values of some material property, and (under some conditions) one might prefer to estimate directly from the data, as in parameterizations three and four, the possibly more basic quantity  $R_0$  rather than  $R$ .

Table 2 shows the results of an extensive MC simulation using LEVM with the usual FPWT weighting[2] for fitting. Values not shown could not be statistically distinguished from zero and had relative standard deviations much greater than unity. Results shown are essentially independent of  $\sigma_r$ , and no relative standard deviations are listed for the linearized estimates because they were all unrealistically small, usually less than  $10^{-4}$ . Nevertheless, we see that there is very little agreement between the linearized MC estimates and the accurate MC ones for the first four parameterizations. For these we see that with  $\psi$  fixed at 0.5 the two free parameters are uncorrelated for all four choices. But when  $\psi$  is also free, high correlation between  $R$  or  $R_0$  and  $\psi$  is evident. In view of the uncertainties of these correlations, there is no strong basis to choose one of these parameterizations over another.

The matter is quite different for parameterizations 5, 6 and 7. Here there is substantial agreement between the first linearized correlation value and the corresponding direct estimate. Furthermore, since these high correlations do not involve  $\psi$ , they persist when it is fixed at 0.5. It thus appears that any of the first four parameterizations is preferable to any of the last three. Furthermore, because of the high value of the MC correlation estimates that is found when  $\psi$  is not fixed, it seems sensible in individual experimental situations to carry out a fit first with  $\psi$  free, then fix it at its estimated value and do another final fitting. Finally, these results should teach one to view linearized correlation values with several grains of salt!

*Miscellaneous IS data-fitting topics*

Although nearly all CNLS fitting minimizes the vector composed of squared, weighted, real and imaginary residuals[1, 2], there has been a small amount of work using a more complicated approach[5, 6] where a  $N \times 2$  rectangular matrix,  $G$ , is formed whose left column involves the unweighted real

Table 1. ZC parameterization choices

No.	A	B	Free parameter choices		Exact parameter values	
			$\theta_1$	$\theta_2$	$\theta_1$	$\theta_2$
1	R	$\tau$	R	$\tau$	1	1
2	R	RC	R	C	1	1
3	$R_0 \sin(\chi)$	$R_0 C_0$	$R_0$	$C_0$	$\sqrt{2}$	$1/\sqrt{2}$
4	$R_0 \sin(\chi)$	$[R_0 \sin(\chi)]C$	$R_0$	C	$\sqrt{2}$	1
5	$\tau/C$	$\tau$	C	$\tau$	1	1
6	$[\tau \sin(\chi)]/C_0$	$\tau$	$C_0$	$\tau$	$1/\sqrt{2}$	1
7	$[\tau_0 \sin(\chi)]/C$	$\tau_0 \sin(\chi)$	C	$\tau_0$	1	$\sqrt{2}$

Here,  $\chi = (\pi/2)\psi$ , and  $Z(\omega) = A/[1 + (i\omega B)^*]$ .

Table 2. Linearized and accurate Monte Carlo correlation estimates for seven different parameterizations of ZC response

No.	Parameters	$\psi$ free		$\psi = 0.5$	
		Linear	MC	Linear	MC
1	$R-\tau$	0.2223	—	0.3938	—
	$R-\psi$	0.3480	0.919 0.005	—	—
	$\tau-\psi$	-0.3536	—	—	—
2	$R-C$	-0.1259	—	0.0099	—
	$R-\psi$	0.3480	0.919 0.005	—	—
	$C-\psi$	-0.4823	—	—	—
3	$R_0-C_0$	0.1095	—	0.0511	—
	$R_0-\psi$	-0.1946	0.80 0.16	—	—
	$C_0-\psi$	-0.3185	—	—	—
4	$R_0-C$	0.1378	—	0.0511	—
	$R_0-\psi$	-0.1946	0.80 0.16	—	—
	$C-\psi$	-0.4823	—	—	—
5	$C-\tau$	0.9392	0.968 0.033	0.9381	0.95 0.060
	$C-\psi$	-0.4823	—	—	—
	$\tau-\psi$	-0.3536	—	—	—
6	$C_0-\tau$	0.9444	0.984 0.013	0.9381	0.95 0.056
	$C_0-\psi$	-0.3185	—	—	—
	$\tau-\psi$	-0.3536	—	—	—
7	$C-\tau_0$	0.9528	0.977 0.024	0.9381	0.95 0.060
	$C-\psi$	-0.4823	—	—	—
	$\tau_0-\psi$	-0.4988	—	—	—

Here  $C|D$  denotes a correlation  $C$  and its relative standard duration,  $D$ .

residuals and whose right column involves the unweighted imaginary residuals. Then the  $2 \times 2$  determinant  $|G_i G_i|$  is minimized, where  $G_i$  is the transpose of  $G$ . Unweighted data fitting results using this multi-response approach have been compared with ordinary CNLS fitting results obtained using LEVM, and completely negligible differences were found[7]. It still remains, however, to compare the utility of the two methods for data which require strong weighting.

The exact small-signal response of a binary electrolyte, one where both positive and negative charges are mobile, cannot be expressed very accurately in terms of an equivalent circuit made up of resistances, capacitances, and any of the ordinary distributed circuit elements[4] used in IS analysis[8, 9]. But the full expression for such response has been incorporated in LEVM and so can be used to fit data obtained from such a system. In a recent paper, many of its possible response shapes are illustrated by means of impedance and admittance plane plots[10]. Under some circumstances, it is found that a shape nearly identical to that for finite-length-Warburg diffusion (or that of Davidson-Cole response[4]) can occur. The degree to which these responses can be discriminated for data without and with random noise is investigated in detail, and it is found that when the noise does not much exceed that usually found experimentally. LEVM allows one to properly identify binary response and discriminate it from the other possibilities.

Finally, a Monte Carlo study of the precision of equivalent-circuit parameter estimates has been carried out using LEVM for several typical IS responses[3]. Not only do these results illustrate the tremendous discrimination possible with CNLS fitting, but they also result in universal curves which can be used to predict the minimum parameter stan-

dard deviations possible for a variety of situations of current interest.

### NEW DEVELOPMENTS IN INTEGRAL-TRANSFORM ANALYSIS OF DISCRETE DATA

#### *Integration errors and random error transformation in Kronig-Kramers transforms*

*Introduction and definitions.* The Kronig-Kramers (KK) dispersion relations (KKR) are important coupled integral transforms connecting the real and imaginary parts of a complex function of frequency,  $F(\omega) = F' + iF''$ , such as an immittance. The conditions which are usually stated[11-15] for the KKR to apply are: causality (*ie* no response before its stimulus is applied), linearity, stability (*ie* time-invariant physical properties), and the real and imaginary parts of  $F(\omega)$  must be finite at  $\omega = 0$  and  $\omega = \infty$  and must be continuous and single-valued functions of  $\omega$  otherwise. Stability and the finiteness of the function at its extremes imply that the properties of the system must lead to passive rather than active response, but property variation slow compared to the measurement time still allows the KKR to apply accurately enough for experimental purposes. The KKR have proved useful for testing the mutual consistency of measured values of  $F'(\omega)$  and  $F''(\omega)$ , for obtaining the other function when only one can be measured, and for examining the stability of corroding electrochemical systems, where property variation usually occurs[11-14, 16]. The linearity condition, which here requires that measured immittance values be independent of the amplitude of the applied voltage, is actually often unnecessary[17, 18].

The KKR connecting  $F(\omega)$  and  $F''(\omega)$  functions which satisfy the above conditions of analyticity, causality, and stability are

$$F'(W) - F'_n = -\left(\frac{2}{\pi}\right)W^{1-n} \times \int_0^\infty \frac{[X^n F''(X) - W^n F''(W)] dX}{X^2 - W^2} \quad (3)$$

and

$$F''(W) = \left(\frac{2}{\pi}\right)W \int_0^\infty \frac{[F'(X) - F'(W)] dX}{X^2 - W^2}, \quad (4)$$

where  $W \equiv \omega\tau_0$  and the value of  $\tau_0$  is arbitrary. When  $n = -1$ , we take  $F'_n \equiv F'(0)$  and set  $F'_n \equiv F'(\infty)$  if  $n = 1$ , the only choice considered here. For discrete data, these integrals must be evaluated by numerical quadrature (see Appendix).

When an analytic expression for  $F(\omega)$  is known but the integrals of equations (3) and (4) cannot be carried out in closed form, intrinsically or because of the presence of noise, again numerical quadrature is required, and one can readily derive the following expressions for the KKR useful in these situations[18],

$$F'(W) - F'_n = \left(\frac{2}{\pi}\right)W^{-n} \times \int_0^1 \frac{[(WY)^n F''(WY) - (W/Y)^n F''(W/Y)] dY}{1 - Y^2} \quad (5)$$

and

$$F''(W) = -\left(\frac{2}{\pi}\right) \int_0^1 \frac{[F'(WY) - F'(W/Y)] dY}{1 - Y^2}. \quad (6)$$

Although there are no poles present in the above forms of the KKR, the limits as  $X \rightarrow W$  and  $Y \rightarrow 1$  require careful evaluation. For  $n = 1$ , it is actually the two parts  $\{F'(W) - F'(\infty)\}$  and  $F''(W)$  which are related by the KKR since the KK transformation of a constant yields zero[19, p. 422].

Dovgii *et al.*[20] have described three error sources in the application of the KKR: (a) the error in the measurement of  $F(\omega)$  or  $F''(\omega)$ ; (b) error arising from the limited frequency range of the measurements; and (c) inaccuracies in the numerical integration required in the transformation. There have been several studies [20] dealing with extrapolation methods used to apply the KKR outside the available range of the measurements and thus to minimize errors of type (b) above; an interesting recent one is that of Esteban and Orazem for low-frequency extrapolation[15]. Although extrapolation of experimental data will usually introduce some error in the transformed results, it can be made small either by extending the measurements to encompass a sufficiently wide frequency range so that contributions from the omitted regions are negligible or by the use of appropriate extrapolation formulas. In the present work we shall either use no extrapolation or accurate noise-free extrapolation contributions.

*Numerical integration errors.* Because noise does not satisfy the KKR, we shall initially consider data

with negligible noise and investigate errors of type (c). Here, I shall first briefly compare integration errors associated with the differing quadrature schemes described in the appendix, then, using MC simulation, explore some of the transformation properties of random errors present in experimental data, type (a) errors.

Although source (c) can be reduced below the range of importance by using sufficient points,  $N$ , in an appropriate quadrature formula, the number of points present in experimental data is usually limited, and it may be impractical to increase it greatly. Alternatively, when the number of available data points is small and limited, increased numerical quadrature accuracy can often be achieved by fitting the data with cubic splines and calculating as many interpolated points as needed, but this procedure may lead to bias in the results. Below, methods will be discussed which allow quite accurate results to be obtained with  $N$  reasonably small.

Detailed results for type-c errors found in KK transformation are listed elsewhere[18]. For the transform of the  $Z'(W)$  of equation (1), with  $B = \tau_0 = 1$  and  $A = \psi = 1$ , (the response of an R and C in parallel), to  $Z''(W)$  for the integration range  $0.1 \leq W \leq 10$ , we found even for  $N$  as small as 18 that the TRAPT procedure defined in the appendix was somewhat superior to GTRAPEI, which, in turn, was somewhat superior to GTRAPGI. But for  $\psi = 0.5$  and the much wider range  $0.001 \leq W \leq 1000$ , TRAPT was usually slightly better than GTRAPEI, and the latter was far superior to GTRAPGI for fixed  $N$ . For example, the relative error found in  $F''(1)$  for 162 function evaluations was  $-3.6 \times 10^{-4}$ ,  $1.2 \times 10^{-3}$  and 3.8, in the same order. It was not until about  $N = 13,000$  that the result for GTRAPEI fell below 1%. Thus in order to obtain adequate accuracy for wide-range data, one can use GTRAPGI with a relatively small value of  $N$  or GTRAPEI with a very much greater value[15].

If one were concerned only with adequate error control for wide-range data smooth in the large, such as that considered here and in the earlier parts of this work, 10–20 evenly spaced points per decade on a logarithmic scale should be quite sufficient for use with GTRAPGI. If the response involved appreciable small-scale structure within one or more decades, one could alternatively, use more geometrically spaced points or split the integral into several parts with appropriate choices of quadrature rule and of  $N$  for each part.

*KK transformation of data errors.* Most errors present in experimental data do not satisfy all the requisite KKR conditions. Thus, close satisfaction of the KKR implies that such errors are negligible. But, of course, this is often not the case for such data. Thus, it is important to examine what happens to KK-transformed data containing errors and to explore ways to reduce the effects of such errors when they might otherwise cast doubt on the applicability of the KKR for a given set of data. Since the effects of data errors in KK transformation have apparently not been previously investigated in quantitative detail[21], it seems worthwhile to do so, especially now that the KKR are finding more exten-

sive use. I summarize here a few of the results of an extensive MC study nearing completion[18].

An analysis of the effects of errors in the original data (type-a) on the KKR requires a MC simulation study in which all other types of errors are minimized. Extrapolation errors were made negligible here by dealing with an analytic function defined over the entire  $0 \leq \omega \leq \infty$  range (here results are only shown for the ZC function of equation (1) with  $\psi = 0.5$  and with the other specific values selected in the last section), and by using exact values of this function for extrapolation outside the limited part of the range where additive or proportional random errors were combined with the exact data, as in equation (2). Numerical quadrature errors were minimized by employing the TRAPT approach of the appendix applied to equations (5) and (6) and using a sufficiently large value of  $N$ .

The MC analysis involves  $K$  replications of the calculation of say  $Z'_m(W)$  [or  $Z''_m(W)$ ], each using  $N$  discrete values of  $Z'_m(X_j)$  [or  $Z''_m(X_j)$ ] with different independent random errors for each value of  $j$  (see equation 2). The  $K$  values obtained for each transform define a distribution for the quantity calculated. One can thus calculate the SD and RSD of the quantity associated with its distribution. Initial numerical calculations led to the surprising but very useful result that such KK transformed SDs were independent of  $N$  for  $N$  large enough to make quadrature errors negligible; thus, the distributions defined by the  $K$  values of the transformed variable were stable for large  $K$ .

The above results suggested that an analytical study of the error effects might be possible and profitable. As shown in [18], it is indeed possible to estimate analytically the KK transformed output values of the SD and RSD, given the form of the input errors and assuming that the integration is ideal (no quadrature errors). Results for the two KK transforms for additive and proportional normally distributed random input errors are presented in Table 3. Surprisingly, we see that transformed SD's are exactly the same as the input ones in these ideal cases! But the output SD/ $\sigma$  and RSD/ $\sigma$  quantities can still show strong dependence on the dimensionless frequency variable  $W$ . Because of the necessity of using numerical integration for experimental data, however, results for the above quantities with finite and relatively small  $N$  values may differ from the ideal predictions[18].

Because achieving adequate accuracy in the KK transforms is harder when  $\psi = 0.5$  in equation (1) than for the narrow-range response obtained with  $\psi = 1$ , only results for the former value are discussed

here, but many others appear in ref. [18]. Furthermore, results are presented here only for proportional data errors. In the MC simulations,  $N$  was usually taken large enough that bias was negligible in the transformed results. Therefore, there was no need to distinguish between such quantities as  $\langle Z'_m(W) \rangle$  and  $Z'_{ex}(W)$ .

After calculating output values of, for example,  $Z''_m$  from input values of  $Z'_m$ , it is useful to plot the three input curves  $Z'_{ex}(W)$  and  $Z'_{ex}(W)[1 \pm \sigma_r]$  and the three resultant curves  $Z''_{ex}(W)$  and  $Z''_{ex}(W)[1 \pm RSD]$ . Figure 1 shows such response over the region  $0.001 \leq W \leq 1000$  where the MC data contain small errors arising from the choice  $\sigma_r = 0.02$ . A value of  $N$  no larger than 200 was needed to achieve accurate results using TRAPT with equation (6), but a much larger value was required for the reverse transform[18]. The response shown in Fig. 1 is in excellent agreement with the predictions of Table 3 for the proportional-error case. At  $W = 0.001$ , the quantity  $RSD/\sigma_r$  was found to be nearly 50, indicating extreme relative error amplification and uncertainty in  $Z''$  in the region where  $|Z''|$  is small. Many more results of the present kind appear elsewhere[18].

*Reduction of impedance spectroscopy data errors by new transformation procedures*

*Background.* Now that we have had a brief look at the KK transformation properties of data errors, it is

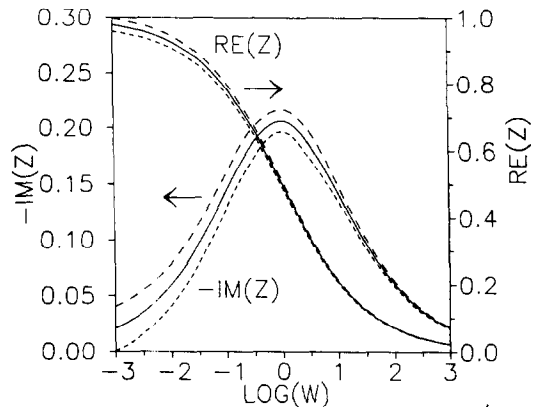


Fig. 1. KK transform from discrete  $Z'$  data with proportional errors having a standard deviation of  $\sigma_r = 0.02$  to  $Z''$  results. For  $Z'_{ex} = 1/[1 + (iW)^{1/2}]$ , input curves are  $Re[Z'_{ex}(W)]$  (solid line) and  $Re[Z'_{ex}(W)][1 \pm \sigma_r]$  (dashed lines), and output curves are  $-Im[Z'_{ex}(W)]$  and  $-Im[Z'_{ex}(W)][1 \pm RSD(W)]$ , where  $W \equiv \omega\tau_0$  and  $RSD(W)$  values were calculated using Monte Carlo simulation involving TRAPT numerical quadrature.

Table 3. Ideal results for the KK transforms of data containing random errors drawn from a normal distribution with zero mean and a standard deviation (SD) of  $\sigma_r$

KK Transform	Error type	Input	Output	Output	
				SD/ $\sigma$	RSD/ $\sigma$
$Im \rightarrow Re$	Additive	$F''(W) \pm \sigma_r$	$F''(W) \pm \sigma_r$	1	$ F''(W) ^{-1}$
	Proportional	$F''(W) \pm \sigma_r F''(W)$	$F''(W) \pm \sigma_r F''(W)$	$ F''(W) $	$ F''(W)/F''(W) $
$Re \rightarrow Im$	Additive	$F'(W) \pm \sigma_r$	$F'(W) \pm \sigma_r$	1	$ F'(W) ^{-1}$
	Proportional	$F'(W) \pm \sigma_r F'(W)$	$F'(W) \pm \sigma_r F'(W)$	$ F'(W) $	$ F'(W)/F'(W) $

time to ask how they can be reduced or eliminated. Here I describe a new transformation method which avoids the arbitrary element present in usual smoothing/filtering techniques and yet yields optimized results. Its background is discussed in [18]. Alternatively, when one is confident that a good choice is available for a function or equivalent circuit with which to fit frequency-response data, CNLS fitting is the method of choice. But when this is not necessarily the case, much can be learned from KK and other transformations. The power of the present approach depends both on its explicit recognition of causality requirements and on smoothing associated with integration[18].

Let us assume that input data,  $F_m(\omega) \equiv F'_m(\omega) + iF''_m(\omega)$  or  $f_m(t)$  are available in either continuous or discrete form. These data may not fully obey the KK relations, may not be entirely causal, and may contain appreciable random noise. We wish to operate on the data in a way which will yield those parts which obey the KKR as closely as possible, which eliminates all or a great deal of the acausal component, and which removes most of the random noise. Such a process is described below and leads to the optimized results  $F_o(\omega) \equiv F'_o(\omega) + iF''_o(\omega)$  and  $f_o(t)$ .

*Analysis.* The four building blocks of the optimization algorithm, which is discussed in more detail and depth elsewhere[18], are as simple as ABC and are

$$\begin{aligned} (\mathcal{A}) \quad f_o(t) &= (1/\pi) \int_0^\infty \text{Re}(F_m(x) \exp(ixt)) dx \\ &= (1/\pi) \{ \mathcal{F}_c[F'_m(\omega)] - \mathcal{F}_s[F''_m(\omega)] \}, \end{aligned} \quad (7)$$

$$\begin{aligned} (\mathcal{B}) \quad F_o(\omega) &= \int_0^\infty f_o(t) \exp(-i\omega t) dx \\ &= \mathcal{F}_c[f_o(t)] - i\mathcal{F}_s[f_o(t)], \end{aligned} \quad (8)$$

$$\begin{aligned} (\mathcal{C}) \quad F_o(\omega) &= \int_0^\infty f_m(t) \exp(-i\omega t) dt \\ &= \mathcal{F}_c[f_m(t)] - i\mathcal{F}_s[f_m(t)], \end{aligned} \quad (9)$$

and

$$\begin{aligned} (\mathcal{D}) \quad f_o(t) &= (1/\pi) \int_0^\infty \text{Re}(F_o(x) \exp(ixt)) dx \\ &= (1/\pi) \{ \mathcal{F}_c[F'_o(\omega)] - \mathcal{F}_s[F''_o(\omega)] \}, \end{aligned} \quad (10)$$

where the right sides show how the relations may be expressed in terms of the sine and cosine integral transforms,  $\mathcal{F}_s$  and  $\mathcal{F}_c$ [19]. These  $\mathcal{A}$ ,  $\mathcal{B}$ ,  $\mathcal{C}$  and  $\mathcal{D}$  relations, applied in various orders, allow one to carry out all needed transformations of given data to an optimized form. Thus  $\mathcal{A}$  transforms frequency response data to optimized time domain response, while  $\mathcal{C}$  transforms time domain data to optimized frequency-domain response.

The sequences  $\mathcal{A}\mathcal{B}$  and  $\mathcal{C}\mathcal{D}$ , respectively, optimize complex frequency-response data and transient-response data. There are some situations where optimization is improved on iteration, such as  $\mathcal{A}\mathcal{B}\mathcal{D}\mathcal{B}\mathcal{D}\mathcal{B}\mathcal{D}\dots$  or  $\mathcal{C}\mathcal{D}\mathcal{B}\mathcal{D}\mathcal{B}\mathcal{D}\mathcal{C}\mathcal{D}\dots$ . The present relations are not equivalent to the usual exponential

Fourier transforms used to pass from the frequency domain to the time domain and *vice versa*. Such transforms provide no optimization; thus, for example, an exponential-Fourier frequency  $\rightarrow$  time  $\rightarrow$  frequency transformation sequence yields an unoptimized output identical to the input. Minor changes in the  $\mathcal{A}$  algorithm allow one to start with either  $F'_m(\omega)$  or  $F''_m(\omega)$  and obtain the optimized results  $F'_o(\omega)$  and  $F''_o(\omega)$ , yielding an optimized form of the KKR. Also because of the discontinuity in a causal  $f(t)$  between  $t = 0 -$  and  $t = 0 +$ , in discrete-data calculations minor corrections to  $f_o(t)$  help to reduce small Gibbs-phenomenon oscillations[18].

*Discussion of optimization results.* Consider exact frequency response data of the form  $F_{ex}(\omega) = R/(1 + i\omega\tau_0) \rightarrow (1 + iW)^{-1}$ , whose exact transient response is  $f_{ex}(t) = (R/\tau_0) \exp(-t/\tau_0) \rightarrow \exp(-T)$ , where we take  $R = 1$ ,  $\tau_0 = 1$  as before, and set  $T \equiv t/\tau_0$ . We shall be concerned with discrete  $F_m(W) = Z(W)$  and  $f_m(T)$  data constructed from  $F_{ex}$  and  $f_{ex}$  with added errors of various kinds. Then the  $\mathcal{A}$  to  $\mathcal{D}$  integrals must be carried out by numerical quadrature. In the following, I have used either GTRAPEI or GTRAPGI. Note that, unlike the usual discrete Fourier transform situation[22], it is not necessary to use the same number of points for time and frequency transform calculations. In fact, given  $N$  measured points for  $F_m$ , for example, one should calculate as many values of  $f_o$ , say  $M$ , using  $\mathcal{A}$ , as needed to allow accurate numerical integration in  $\mathcal{B}$ , possibly a considerably larger or even smaller number than  $N$ .

Figure 2 shows complex-plane  $\mathcal{A}\mathcal{B}$  optimization results when an acausal damped exponential is added to the exact data. For this analysis,  $N$  was 1024 and the minimum and maximum values of  $W$  were 0 and  $50\pi$ , so no extrapolation was needed. Very similar results were obtained using only 128 points with  $W_{max} = 4\pi$  and high-frequency extrapolation for larger  $W$ . The method of plotting employed in Fig. 2 and in subsequent figures allows one to see not only how well the shape of the optimized result curve,  $Z_o(W)$ , approximates that of the  $Z_{ex}$  part of the data, but also how well the frequency response agrees. If the solid points fall exactly in the middle of the exact square-box points, optimization

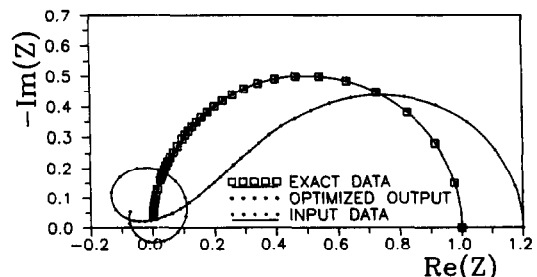


Fig. 2. Complex plane plots of the optimizing transform of single-time-constant input data with acausal systematic error:  $Z = Z_m = [1 + iW]^{-1} + \epsilon \exp[(\pi/9)\{-0.1|W| + iW\}]$ , with  $\epsilon = 0.2$ ,  $W \equiv \omega\tau_0$ , and the numerical value of  $\tau_0$  taken to be unity. The calculations were carried out with  $N = 1024$  and the squares are centered at exact data values. In this and subsequent figures, lines between the discrete points have been included only to guide the eye.

is perfect. Here, we see that it is exceptionally good over the full frequency range shown and that the part of the input data which does not satisfy the KKR has been eliminated.

Figure 3a presents input data with proportional random errors for the real and imaginary parts drawn from independent normal distributions with zero means and with standard deviations,  $\sigma_r$ , of 0.1, appreciably larger than usual experimental errors. Results of the  $\mathcal{A}$  transformation of these  $N = 128$  data points appear in Fig. 3b and demonstrate much smoothing. The unimportant deviations from the exact response at large  $T$  approach zero as  $N$  increases and/or  $\sigma_r$  decreases toward zero. Finally, Fig. 3c shows the results of the  $\mathcal{B}$  transformation using  $M = 351$ ; for clarity not all optimized points are included. Although the optimized  $Z(W)$  values are not perfect, they clearly agree far closer with the exact response than do the input values. Thus, the signal-to-noise factor has been greatly increased by the optimization. Accurate extrapolation was used here for  $W > 4\pi$ . Even better results are obtained with larger  $N$  values. With  $\sigma = 0.1$  and additive rather than proportional errors present, much larger input errors are present in the high-frequency region, and optimization error reduction is large but not so close to perfection in this region. With error-free input data, the  $f_0(T)$  and  $Z_0(W)$  optimized outputs are indistinguishable from  $f_{ex}(T)$  and  $Z_{ex}(W)$ , respec-

tively, when  $N$  is sufficiently large [ $ie \geq 100$  for  $f_0(T)$  here and even less for  $Z_0(W)$ ].

Figure 4 shows  $\mathcal{C}$  time  $\rightarrow$  frequency optimization results starting with  $M = 351$  random errors with  $\sigma_r = 0.1$ . These errors are added proportionately to the exact response,  $f(T) = \exp(-T)$ , where  $T \equiv t/\tau_0$  and  $\tau_0 = 1$  s as usual. No  $T$  extrapolation was needed here. Although the input noise does not appear large, this is because it is plotted on a logarithmic scale. The exact time domain response, and this response with noise, are presented in Fig. 4a, and the resulting optimized frequency response with  $N = 512$  appears in 4b. Finally, the results of Fig. 4c show that the original transient-response noise is almost entirely eliminated from the optimized response. But, unlike  $\mathcal{A}\mathcal{B}$  optimization, we start with causal data here; thus there is no causal filtering and that apparent for  $f_0$  is a filtering effect primarily associated with the finite value of  $W_{max}$  used. Here  $W_{min} = 0.03\pi$  and  $W_{max} = 4\pi$ . When  $W_{max}$  remains at this value but no extrapolation is used for larger  $W$ , the resulting  $f_0(T)$  curve is smooth but contains appreciable oscillations which increase with increasing  $T$ . On the other hand, when there is again no large- $W$  extrapolation but  $W_{max}$  is increased to  $25\pi$  or more,  $f_0$  is nearly indistinguishable from  $f_m$ . In all of these situations, however,  $F_0$  remains close to  $F_{ex}$ , as in Fig. 4b, and becomes closer and closer to  $F_{ex}$  as  $M$  increases.

Since the KK relations with  $n = 1$  apply to the combination  $Z(\omega) - Z(\infty)$ , rather than to just

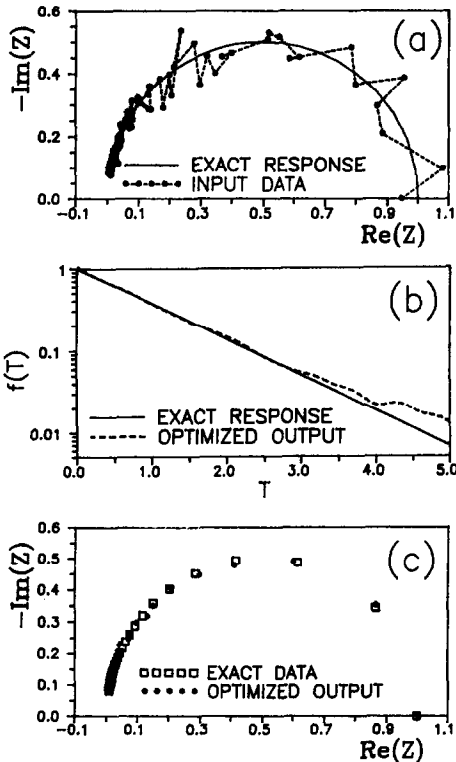


Fig. 3. Results of  $\mathcal{A}\mathcal{B}$  optimization of  $Z = [1 + iW]^{-1}[1 + \text{random noise with zero mean and } \sigma_r = 0.1]$ . Part (a) is a complex plane plot of the noisy input data; part (b) shows the corresponding optimized time response with  $T = t/\tau_0$ ; and part (c) presents the final optimized frequency response.

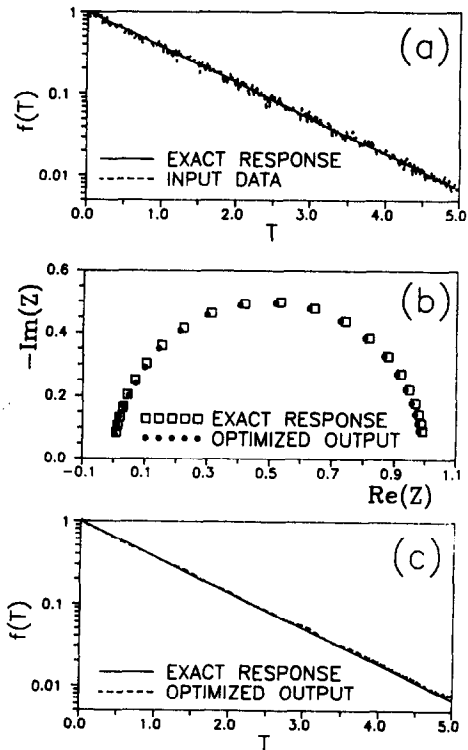


Fig. 4. Results of  $\mathcal{C}$  optimization of the noisy time response  $f(T) = \exp(-T)[1 + \text{random noise with zero mean and } \sigma_r = 0.1]$ , where  $T \equiv t/\tau_0$ . Part (a) shows the noisy input data points; (b) shows the corresponding optimized frequency response; and part (c) presents the final optimized transient response.

$Z'(\omega)$ , it is reasonable to ask whether the optimizing transformation can properly handle data for which  $Z'(\infty)$ , eg bulk or wiring resistance, is non-zero. To find out, I generated 128 data values from  $Z(W_j) = (0.5 + [1 + iW_j]^{-1} + (\text{independent random errors with } \sigma_r = 0.1))$  for the range  $0.03\pi \leq W \leq 4\pi$ . Here full convergence required 665 iterations but led to complete elimination of the 0.5 offset as well as great reduction in the original noise. Full convergence was achieved with only 185 iterations when  $\sigma_r$  was taken zero, but in either case only slight improvement was found after about 100 iterations. In actual practice, one would usually have available a reasonably good estimate of  $Z'(\infty)$ , which could be subtracted from the data before optimization. Then optimization would allow one to further refine the initial value of  $Z'(\infty)$  and to greatly reduce errors, both random and acausal. Although  $\mathcal{A}\mathcal{B}$  optimization results are not shown here when only imaginary or real data values are used as input [see 18], values of  $F'_0(\omega)$  and  $F''_0(\omega)$  are found from such optimization which are very nearly as satisfactory as those of Fig. 3c.

### SUMMARY

The present results demonstrate the power of the optimizing transformation to carry out KK transforms, to do the work of ordinary Fourier transforms, and, at the same time, to largely eliminate random errors and some systematic errors. It is worth again emphasizing that the present  $\mathcal{A}\mathcal{B}$  optimization procedure is not a traditional smoothing/filtering approach, but one which can usually accomplish the same task better and more objectively since there is no need to select a particular filter high-frequency cut-off limit or a specific degree of smoothing. Although the present results were calculated using data that become negligibly small within a relatively narrow frequency range, the same optimization technique is applicable for data involving one or more different physical processes and covering a frequency range of many decades, provided that the numerical integration required is carried out sufficiently accurately.

*Acknowledgement*—The many useful suggestions of Professor William J. Thompson are greatly appreciated.

### REFERENCES

1. J. R. Macdonald (Ed.), *Impedance Spectroscopy—Emphasizing Solid Materials and Systems*. Wiley-Interscience, New York (1987).
2. J. R. Macdonald, *Electrochim. Acta* **35**, 1483 (1990).
3. J. R. Macdonald, *J. electroanal. Chem.* **307**, 1 (1991).
4. R. L. Hurt and J. R. Macdonald, *Solid State Ionics* **20**, 111 (1986).
5. S. Havriliak, Jr. and D. G. Watts, in *Design, Data, and Analysis* (Edited by C. L. Mallows). John Wiley, New York (1987).
6. D. M. Bates and D. G. Watts, *Nonlinear Regression Analysis and its Applications*. John Wiley, New York (1988).
7. J. R. Macdonald, *Solid State Ionics* **58**, 97 (1992).
8. J. R. Macdonald and D. R. Franceschetti, *J. chem. Phys.* **68**, 1614 (1978).
9. J. R. Macdonald, *J. electrochem. Soc.* **135**, 2274 (1988).

10. J. R. Macdonald, *Electrochim. Acta* **37**, 1007 (1992).
11. D. D. Macdonald and M. C. H. McKubre, in *Impedance Spectroscopy—Emphasizing Solid Materials and Systems* (Edited by J. R. Macdonald), pp. 154, 274–275, 311. Wiley-Interscience, New York (1987).
12. D. D. Macdonald and M. Urquidi-Macdonald, *J. electrochem. Soc.* **132**, 2317 (1985).
13. M. Urquidi-Macdonald, S. Real and D. D. Macdonald, *J. electrochem. Soc.* **133**, 2018 (1986).
14. D. D. Macdonald and M. Urquidi-Macdonald, *Corrosion* **45**, 327 (1989).
15. J. M. Esteban and M. E. Orazem, *J. electrochem. Soc.* **138**, 67 (1991).
16. H. Shih and F. Mansfeld, *Corros. Sci.* **28**, 933 (1988).
17. F. Bassani and S. Scandolo, *Phys. Rev. B* **44**, 8446 (1991).
18. J. R. Macdonald and W. J. Thompson, work in progress.
19. J. R. Macdonald and M. K. Brachman, *Rev. Mod. Phys.* **28**, 393 (1956).
20. Y. O. Dvoggii, M. K. Zamorskii and I. V. Kityk, *Soviet Phys. J.* **32**, 175 (1989).
21. B. D. O. Anderson and M. Green, *IEEE Trans. Circuits Syst.* **35**, 528 (1988).
22. W. H. Press, B. P. Flannery, S. A. Teukolsky and W. T. Vetterling, *Numerical Recipes*, pp. 387–395. Cambridge University Press, New York (1986).

### APPENDIX

Although an experimenter can usually select the  $X_j$  or  $Y_j$  values used in discrete approximations of equations (3) to (6), and often chooses values separated by a constant increment, this choice is inappropriate for data extending over many decades of  $X$  since it requires an excessively large value of  $N$  to achieve adequate accuracy. See, for example, the work of [15]. Furthermore, one sometimes needs to analyze data with variable intervals. To do so, I have developed and found particularly useful the following generalized trapezoidal quadrature procedure, GTRAP. It is appropriate for arbitrary  $X_j$  spacing, and is expressed as

$$I = \int_{X_1}^{X_N} h(X) dX \approx \sum_{j=1}^N w_j h(X_j), \quad (\text{A1})$$

where  $h(X)$  is any appropriate function, and the  $w_j$  are the quadrature weights, the crucial element in the procedure. They are given by

$$w_1 = \frac{1}{2}[X_2 - X_1], \quad (\text{A2})$$

$$w_j = \frac{1}{2}[X_{j+1} - X_{j-1}], \quad (1 < j < N), \quad (\text{A3})$$

and

$$w_N = \frac{1}{2}[X_N - X_{N-1}]. \quad (\text{A4})$$

The approximation in equation (A1) is actually exact when  $h(X)$  is a first-degree polynomial in  $X$  and reduces to the ordinary closed, extended trapezoid rule [22, pp. 107–111] for equal increments (EI) in  $X_j$ : GTRAPEI.

For reasonably smooth data, extending over a wide range of  $X$ , say several decades or more, (such as the responses considered herein), it is generally more efficient to use geometric intervals (GI) in  $X_j$  rather than EI. Then one might choose, for example,

$$X_{j+1}/X_j = [X_N/X_1]^{1/(N-1)}, \quad (\text{A5})$$

with  $X_1 \neq 0$ , resulting in the procedure GTRAPGI.

Because of the narrow range in  $Y$  of equations (5) and (6), GTRAPEI may be used for a discrete quadrature approximation to them. We [18] have actually used the open midpoint generalization of the trapezoidal integration rule with equal increments [22, pp. 116–117] for the MC study of KK noise transformation. This combination, for equations (5) and (6), is designated TRAPT.